Human Movement Science 11 (1992) 239–251
North-Holland

Biomechanical and haptic factors in the temporal patterning of limb and speech activity *

Elliot L. Saltzman

Haskins Laboratories, New Haven, USA and University of Connecticut, Storrs, USA

Abstract

Saltzman, E.L., 1992. Biomechanical and haptic factors in the temporal patterning of limb and speech activity. Human Movement Science 11, 239–251.

This paper describes two ways in which events occurring in the peripheral musculoskeletal apparatus can shape or alter the temporal structure of ongoing movements. First, the biomechanical properties of a simulated, two-joint arm are shown to play a formative role in the creation of rhythmic, modal movement patterns. These patterns are interpreted as mutual entrainment phenomena between a pair of (highly) nonlinear oscillators. Second, peripheral haptic information has been shown in preliminary phase-resetting analyses to modulate the timing structure of rhythmic speech sequences. Implications of both sets of results for understanding the acquisition and performance of skilled movements are discussed briefly.

Introduction

The peripheral musculoskeletal apparatus influences and shapes motor performance in many ways. Kinematically, it defines the geome-

* The work reported in this paper was supported by grants to Haskins Laboratories from the following sources: NIH Grant NS-13617 (Dynamics of Speech Articulation) and NSF Grant BNS-8520709 (Phonetic Structure Using Articulatory Dynamics). The contributions of Patrick Haggard, Scott Kelso, and Kevin Munhall to the collection and analysis of data from several pilot studies are gratefully acknowledged, as are comments on earlier drafts of this manuscript by Eric Vatikiotis-Bateson, Vincent Gracco, Bruce Kay, Philip Rubin and Michael Turvey. Finally, I would like to thank Alice Faber, Yvonne Manning, Philip Rubin, and Caroline Smith for their assistance with figure preparation.

Author's address: E.L. Saltzman, Haskins Laboratories, 270 Crown Street, New Haven, CT 06511, USA.

try of interaction between actors and their external gravitational and mechanical environments. Relatedly, it defines structured efferent and afferent transactions with the haptic array in which the actor is embedded. Finally, it comprises a complex dynamical system whose properties cannot be ignored during the performance of skilled actions. This paper describes two aspects of temporal patterning in skilled movements that are related to these properties of the musculoskeletal apparatus. The first topic concerns the possible formative roles of peripheral biomechanics in shaping the temporal patterns of multi-joint, rhythmic limb movements. The focus of this discussion is on simulations of a biomechanically simple two joint arm. The second topic concerns the manner in which information from the mechanical periphery is integrated into the real-time temporal structuring of speech, and focuses on preliminary phase-resetting data collected during the production of repetitive speech sequences.

Simulated limb movements: Formative biomechanical influences

Several years ago, when developing a computational, *task-dynamic* model of skilled limb activities (Saltzman and Kelso 1987), I explored the results of applying time-invariant dynamics directly to the biomechanical degrees of freedom of a simple, 2-joint simulated arm. At the time, my main interest was in contrasting the arm's reaching or targeting behavior when governed by point attractor dynamics specified at the levels of either joint-angle coordinates (articulatory space) or task-specific, end-effector coordinates (task space). The simulations demonstrated that, although the target was attained by the hand in both cases, only the task-dynamic method gave a good approximation of the hand's spatial path en route to the target. A similar conclusion, not reported in Saltzman and Kelso (1987), was reached from simulations of rhythmic tasks in which invariant limit cycle dynamics were specified at the levels of either articulatory or task space coordinates. The patterns produced by articulator-level limit cycle dynamics were not well suited to performing rhythmic tasks that are directed spatially toward surfaces and objects in the real world, such as polishing a car or mixing spaghetti sauce in a bowl. The task-dynamic approach worked much better (see, for example, the rhythmic reaching simulation in Saltzman and Kelso 1987).

Several aspects of the articulator-dynamic rhythmic simulations were intriguing, however, in that they illustrated the potentially formative role of 'passive' biomechanical properties in shaping a limb's observable movement patterns. In these simulations, the intrinsic biomechanical behavior of the 2-joint arm (planar; no gravity; frictionless hinge joints with 'shoulder' and 'elbow' angles θ_1 and θ_2; 'upper arm' and 'forearm' segments defined as thin rods with lengths l_1 and l_2, and with masses m_1 and m_2 uniformly distributed along the segment lengths) was augmented by limit cycle controllers defined separately at each joint, as described by the following equation of motion (see Saltzman (1979) and Saltzman and Kelso (1987) for further details):

$$M\ddot{\theta} + S\dot{\theta}_p = -K\Delta\theta - \tau_e, \tag{1}$$

where

$M = M(\theta)$, the 2×2 *acceleration sensitivity matrix* associated with intrinsic inertial torques, whose elements, q_{ij}, are functions of the current linkage configuration, θ, and where $q_{11} = m_2(l_1^2 + (1/3)l_2^2 + l_1 l_2 \cos \theta_2) + m_1(1/3)l_1^2$; $q_{12} = m_2((1/3)l_2^2 + (1/2)l_1 l_2 \cos \theta_2)$; $q_{21} = q_{12}$; $q_{22} = m_2(1/3)l_2^2$; and $m_1 = 1.05$ kg, $m_2 = 1.25$ kg, $l_1 = 0.32$ m, $l_2 = 0.38$ m;

$S = S(\theta)$, the 2×2 matrix associated with intrinsic coriolis torques (related to joint velocity products) and centripetal torques (related to squares of joint velocities), whose elements, s_{ij}, are functions of the current linkage configurations, θ, and where $s_{11} = 0$; $s_{12} = -m_2 l_1 l_2 \sin \theta_2$; $s_{13} = (1/2)s_{12}$; $s_{21} = -s_{13}$; $s_{22} = 0$; $s_{23} = 0$;

$\theta_p = (\dot{\theta}_1^2, \dot{\theta}_1\dot{\theta}_2, \dot{\theta}_2^2)^T$, the current joint velocity product vector;

$K =$ the 2×2 diagonal stiffness control matrix, where $k_{11} = k_{22} = 10.0$; $k_{12} = k_{21} = 0.0$;

$\Delta\theta = \theta - \theta_0$, where $\theta_0 =$ the 2×1 rest configuration control vector whose elements, θ_{0i}, are the rest angles for the shoulder and elbow, and are varied across different simulation trials;

$\tau_e =$ the 2×1 nonlinear escapement control vector (*Rayleigh*-type; e.g., Kay et al. 1987; Beek 1989; Beek and Beek 1988), whose elements, τ_{ei}, are functions of the current joint velocities, and $\tau_{ei} = \alpha_i\dot{\theta}_i + \beta_i\dot{\theta}_i^3$, where $\alpha_i = -2.0$ and $\beta_i = 0.025$.

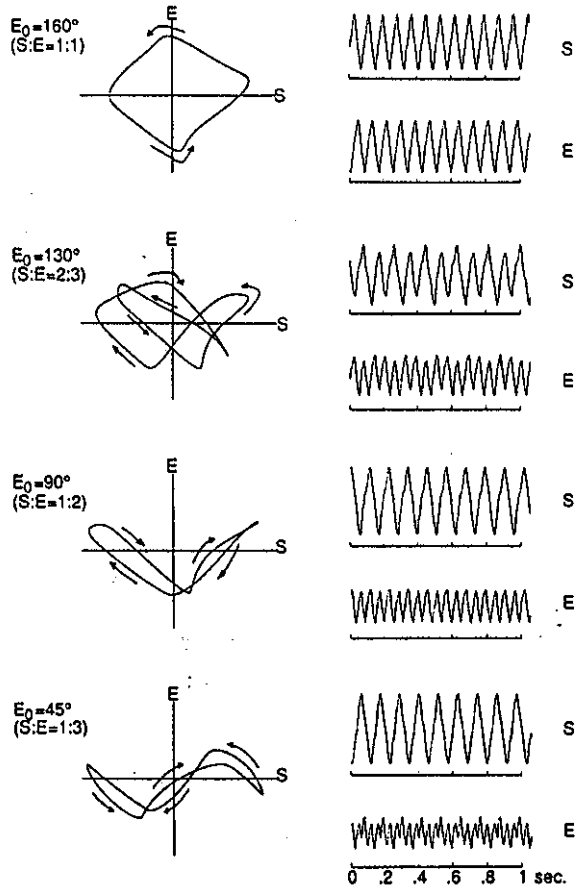

Fig. 1. Lissajous (left column) and time series (right column) trajectories for simulated 2-joint arm. S = Shoulder, E = Elbow, E_0 = Elbow rest angle (see text for further details).

In all simulations, all parameters were held constant across simulation trials, except for the rest configuration of the arm, θ_0. Fig. 1 shows the post-startup, steady-state movement patterns for a subset of these trials at different settings for elbow rest angle ranging from 45° (bottom row) to 160° (top row) across trials, with shoulder rest angle held constant at 90°. In the left column the movements are displayed as Lissajous (angle-angle) diagrams, centered on the rest configuration for the displayed trial; on the right are the corresponding time series. In all cases shown, simulations were started at the initial conditions

$\theta = 0$ and $\dot{\theta} = 0$, and the different movement conditions could be characterized by the resultant ratio of the number of shoulder cycles to the number of elbow cycles (S:E). What is most remarkable is the richness of stable temporal patterns that was found for this extremely simple control parameter manipulation. [1] How do these patterns arise, what is the source of their stability, and what role does elbow rest angle play in shaping the observed cycle ratio patterns? In order to address these specific questions more fully, let us first briefly review how these types of rhythmic entrainment phenomena are treated in the general domain of qualitative (nonlinear, dissipative) dynamics (e.g., Abraham and Shaw 1982, 1986; Thompson and Stewart 1986).

A limit cycle oscillator displays stable rhythmic motion whose amplitude and frequency are dependent on the oscillator's dynamic characteristics, e.g., its mass, stiffness, and escapement (i.e., linear and nonlinear damping) properties. When two roughly similar limit cycles are coupled together so that the motions of each oscillator perturb one another, even weakly, the oscillators typically enter into either of two higher order, *modal* states of 1-1 mutual entrainment. For example, when two nearly identical oscillators are coupled together so that each component experiences a weak perturbing force that depends linearly on the position of the other (i.e., via a coupling term $\gamma_{ij}\theta_j$, from component-j to component-i) the coupled system displays one mode in which the components are constantly in phase (phase-locked at 0° phase difference) and another mode in which they are constantly out of phase (180° phase locking). The particular mode or entrainment regime that is 'selected' will depend on the initial conditions (initial positions, velocities) of the two individual oscillatory components. In each 1-1 modal state, the components oscillate at a mode-specific common frequency, and display a mode-specific amplitude ratio and interoscillator phase difference (possibly different than either 0° or 180°). In general, neither the amplitudes nor the

[1] Additional patterns, some more complicated than those displayed in fig. 1, were found for other values of elbow rest angle starting from the same initial conditions ($\theta = 0$ and $\dot{\theta} = 0$). e.g., a 3:4 ratio for shoulder:elbow freqency when elbow rest angle equals 135°. Further, some parameterizations showed an additional stable pattern that was reached after starting from different initial conditions, e.g., for elbow rest angle = 160°, a 1-1 ratio exhibiting a *clockwise* orbit on the Lissajous plane was attained after starting from $\theta = \theta_0$ and $\dot{\theta} = (0, 200)^T$.

frequencies displayed in the entrained state need necessarily match the natural frequencies and amplitudes of the component oscillators in isolation.

When the ratio of the components' natural frequencies is roughly that of two *relatively prime* small integers $m:n$ (i.e., ratios where m and n have no common factors except 1, such as 1:2, 2:3, 3:4, 2:5, etc.), the system typically settles into an entrainment regime (subharmonic or superharmonic) in which the two components oscillate at exactly that integer frequency ratio (e.g., Linkens 1983). Adopting the convention $m \leq n$, where m and n refer to the slower and faster component oscillators, respectively, a coupled system can be said to define a single higher-order periodic interval for every m and n cycles of the slow and fast components, respectively. The intercomponent phase difference, $\Delta\phi$, is not stationary, as it is in the case of stable 1-1 entrainment, but rather drifts at a constant rate that is linearly proportional to the intercomponent frequency difference, Δf, i.e., $(d/dt)\Delta\phi = 2\pi(\Delta f)$. However, a given $m:n$ ratio can be exhibited in different movements patterns that are distinguishable by the particular intercomponent phase differences shown at a given temporal proportion of the global, higher-order periods.

These considerations allow us to understand more fully the processes giving rise to the movement patterns shown in fig. 1. The first lesson is that even very simple coupling between two limit cycle oscillators can give rise to temporally structured, modal behaviors. My initial reaction to seeing stable integer-ratio entrainment in the arm simulations was one of surprise, since I had not explicitly coupled the limit cycle controllers, and limit cycles will not entrain without coupling. However, it soon became clear that the limit cycles were coupled implicitly through the reactive inertial, centripetal, and coriolis torques of the arm's intrinsic biomechanics. Thus, the simulations underscore the potentially formative role of reactive phenomena in shaping the temporal structure of movement patterns. This point is consistent with Bernstein's (1967/1984) hypothesis that at the highest stages of skill development 'the organism is not only unafraid of reactive phenomena in a system with many degrees of freedom, but is able to structure its movements so as to *utilize entirely the reactive phenomena* which arise' (p. 109/217).

The second lesson to be gained from our earlier discussion of oscillator theory concerns why the frequency ratios displayed in fig. 1

were dependent on the dynamic parameter of elbow rest angle but not, as it turned out, on shoulder rest angle. What is so special about elbow rest angle that it should so strongly influence the simulated arm's modal patterns? Oscillator theory tells us that, when the natural frequencies of coupled limit cycles are 'close enough' to integer ratios of one another, the components can mutually entrain one another at exactly that ratio. In a set of coupled oscillators, the intrinsic frequencies of the components can be determined from the linearized *system matrix*, $Y = M^{-1}K$, where M and K are the system's inertia and stiffness matrices, respectively (e.g., Thomson 1981). The uncoupled natural frequency of the ith component, ω_{oii} (rad/sec), can be computed from Y's diagonal element, $y_{ii}, = (\omega_{oii})^2$; and linearization occurs with respect to the system's static equilibrium configuration. From eq. (1), it can be seen that the M-matrix is a function of elbow angle but not shoulder angle. Further, since the system's static equililibrium configuration is equal to its rest angle vector, we can see that the uncoupled natural frequencies of the 'component' shoulder and elbow oscillators will be functions of elbow, but not shoulder, rest angle. For the cases shown from top to bottom in fig. 1, the ratios of ω_{oS}/ω_{oE} computed from the Y-matrix are 0.86, 0.67, 0.52, and 0.43. The values clearly scale with the value of elbow angle, and track the values of the shoulder-to-elbow frequency ratios actually observed: 1.0, ~ 0.67, 0.50, and ~ 0.33. Thus, these simulation data suggest that a possible role for static equilibrium configuration (i.e., rest configuration, θ_0) in multijoint rhythmic tasks may be the harnessing of pattern-forming properties (modal dynamics) that are intrinsic to selected regions of the workspace.

In summary, our considerations of oscillator theory in the context of simulated movements of a simple 2-joint arm have led us to the viewpoint that the 'passive' biomechanical properies of a limb (reactive coupling; configuration-dependent inertial properties) may shape the movement patterns of a given articulatory system, at least during the performance of rhythmic tasks. Echoing Bernstein (1967/1984), we note the possibility that this formative power may be exploited at the highest levels of skill acquisition, when and if it fosters the growth of modal patterns that are compatible with the constaints and goals of an intended task. Further, we have shown that this formative power may be harnessed by very simple manipulations of dynamic control parameters.

Temporal patterns in speech: Effects of mechanical perturbations

What is the role of proprioceptive/haptic information in shaping the underlying temporal structure of complex skills such as speaking or tying one's shoes? Recent data on unimanual oscillatory movements (Kay 1986; Kay et al. 1991) has demonstrated that transient mechanical perturbations delivered to the motor periphery induce permanent and systematic shifts in the phasing of such rhythmic movements. Gracco and Abbs (1989) have shown that similar perturbations during single, noncyclic productions of 'sapapple' have the effect of inducing systematic shifts in the timing or phasing of subsequent movement elements. However, since these speech data are from short sequences, it is not possible to determine if the perturbation actually reset an underlying sequence 'clock', or if the temporal shifts were due to systematic effects in the articulators' transient, post-perturbation behavior. In order to distinguish between these two possibilities, my colleagues and I have been conducting a *phase-resetting* experiment on the production of extended, repetitive speech sequences (Saltzman et al., in preparation).

The goal of phase resetting analyses (e.g., Glass and Mackey 1988; Kawato 1981; Winfree 1980) is to determine whether perturbations delivered during an ongoing rhythm have a permanent effect (i.e., phase shift) on the underlying temporal organization of the rhythm. Such techniques have been applied in numerous neurophysiological and kinematic studies of the motor control mechanisms that generate rhythmic movements (e.g., Lennard and Hermanson 1985; Lee and Stein 1981). What is measured in such studies is the amount of temporal shift introduced by the perturbation, relative to the sequence's timing prior to the perturbation. This phase shift is measured after the perturbation-induced transients have subsided and the system has returned to its pre-perturbation, steady-state rhythm. If the perturbation induces such a shift in an extended, repetitive speech sequence, this result would place a major constraint on theories of speech production that posit a central timing network or 'clock' underlying the production of such sequences (e.g., Saltzman and Munhall 1989). Such a result would imply that the hypothesized central timekeeper could not simply drive the articulatory periphery in a strictly feedforward, unidirectionally coupled manner. Rather, the hypothesized central timer and the peripheral musculoskeletal appa-

ratus must be coupled bidirectionally, so that feedback information concerning the biomechanical state of the periphery can influence the functioning of the timer.

Methods

Subjects and equipment

In this experiment, a single subject was seated in an adjustable dental chair, with his head restrained in an external frame. A small paddle connected to a torque motor was placed on the lower lip with a tracking force of 3 gm, in order to deliver step pulses of downward force (50 gm) at random times during the experimental trials. Timing of perturbation onset was controlled by a VAXstation II/GPX. Infrared light-emitting diodes were mounted on the upper lip, lower lip, lip paddle, jaw, nose (the nose LED acted as a spatial reference), and movements were measured optoelectronically. Additionally, the acoustic speech signal and control voltage applied to the torque motor were recorded. All data was fed into a 16 track FM tape recorder for later digitization.

Protocol

Two experimental sessions were conducted, each lasting approximately 3 hours, and 12 blocks of 25 trials were performed per session. Blocks alternated between *repetitive* and *discrete* experimental conditions. In the discrete condition, each trial consisted of the single 'word' /pəsæpæpl/ (pronounced 'puhsapapple'); in the repetitive condition, each trial consisted of a sequence of approximately 15–20 repetitions of the syllable/pæ/(pronounced 'paa'), spoken at a syllable rate comparable to that used in the discrete trials. Perturbations were delivered during a random sampling of 80% of the trials; perturbation duration was preset in an external timing circuit to equal the subject's average syllable duration during repetitive trials measured prior to the beginning of data collection. To date, only the repetitive condition has been analyzed. On each perturbation trial of this condition, the perturbation was delivered during the nth syllable (n varied randomly from 8–11), and after m% of the predetermined syllable duration (m varied randomly from 1–100). Task instructions were to not actively resist the perturbation, and to return to a steady

rhythm similar to that produced before the perturbation as quickly and easily as possible.

Results

For each perturbation trial, a lip-aperture (LA) trajectory was defined by subtracting the upper lip signal (UL) from the lower lip signal (LL), i.e., LA = LL − UL (fig. 2 illustrates LA trajectories from two perturbation trials). Individual cycles were then defined between successive peak bilabial openings, and four cycle types were identified: (a) *pre-perturbation* cycles included the trial's first cycle through the last cycle prior to the one containing the perturbation onset; (b) *perturbation* cycles included all cycles that overlapped the perturbation interval; (c) *transient* cycles were defined as those cycles following the perturbation during which cycle periods deviated from the average pre-perturbation cycle period by more than an absolute-valued percentage criterion (this criterion was set on a trial-by-trial basis to

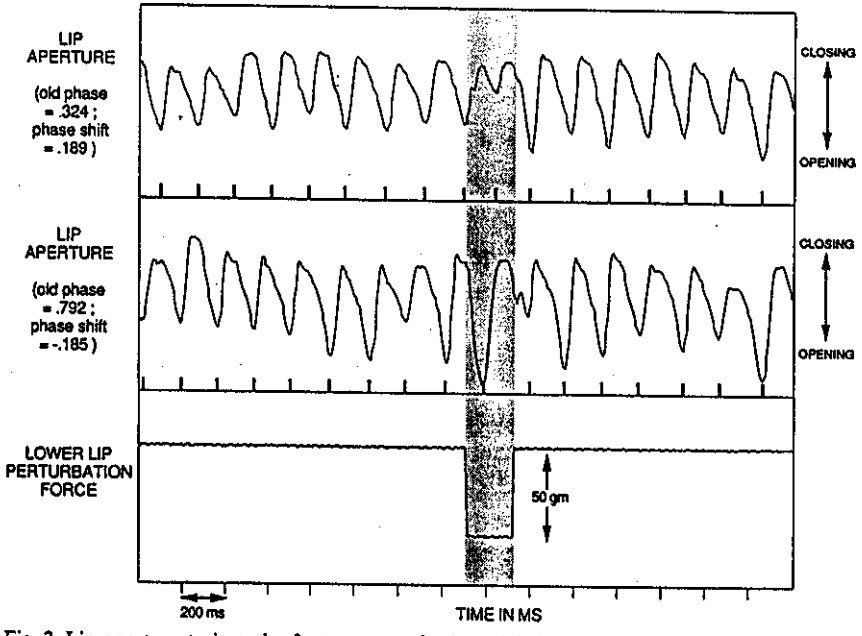

Fig. 2. Lip aperture trajectories for two perturbation trials in which perturbation offsets defined an old phase of 0.324 (top row) and 0.792 (middle row). A time-aligned trajectory for lower lip perturbation force is shown in the bottom row.

equal the absolute value of the largest percentage deviation of the pre-perturbation cycles from their own average period); and (d) *post-return* cycles were defined from the last transient cycle to the end of the trial.

Cycle phase, ø, was defined to be zero at all peak bilabial openings. For all other points between peak openings, phase was defined as (t/T_i), where t is the time (in sec) from the most recent peak preceding a given event of interest, and T_i is the period (in sec) of the cycle containing the event. The phase of perturbation delivery was defined with respect to the time of perturbation offset. This offset time served as a temporal anchoring point for 'strobing' both backward and forward in time into the pre-perturbation and post-return cycle sequences, respectively, using the average pre-perturbation cycle period to define the strobe period. The within-cycle strobe phases from the pre-perturbation and post-return cycles were then averaged to define an *average old phase*, $\overline{\phi}_{old}$, and *average new phase*, $\overline{\phi}_{new}$, respectively. *Phase shift*, $\Delta\phi$, was then defined as $(\overline{\phi}_{new} - \overline{\phi}_{old})$ (modulo 1). Thus, $\Delta\phi$ is the amount that a given trial's post-return rhythm has been shifted relative to its pre-perturbation rhythm ($\Delta\phi > 0$ denotes phase advance; $\Delta\phi < 0$ denotes phase delay). The same measures were obtained for the control (no perturbation) trials, where calcula-

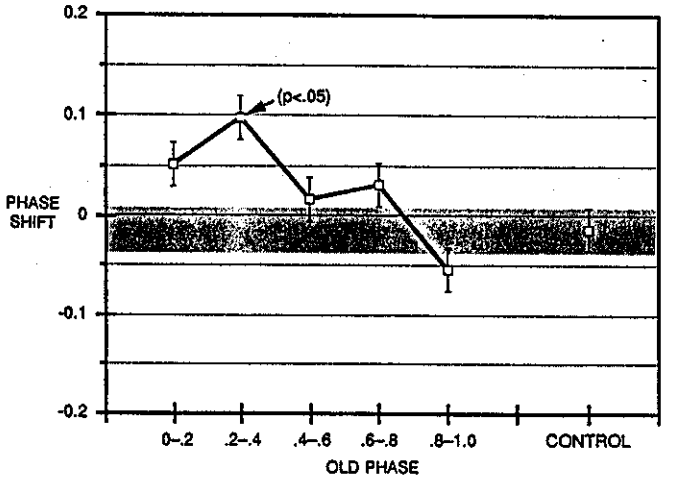

Fig. 3. Summary of phase shift data. Number of trials included in bins, from left to right, are 42, 34, 34, 33, 32, 52. (Open squares = bin means. Vertical bars = standard errors.)

tions were anchored to the end of a randomly timed, but not delivered, 'perturbation'.

Fig. 3 illustrates the results of our analyses (one subject, two sessions), using data binned according to intervals of old phase. As can be seen in the figure, the rhythm showed a phase shift in the 0.2–0.4 interval that was significantly different from the no-perturbation control trials (Dunnett's test, $p < 0.05$). Thus, although preliminary, these data support the hypothesis that central timing processes for speech are indeed affected by haptic events experienced at the biomechanical periphery, and that such events can permanently reset the rhythms of such central 'clocks'.

Conclusions

This paper has highlighted several of the ways in which events occurring in the peripheral musculoskeletal apparatus can shape or alter the temporal structure of ongoing movement patterns. The biomechanical properties of a simulated arm were shown to play a formative role in the creation of rhythmic, modal movement patterns. It is possible that such processes may facilitate or interfere with the performance or learning of these types of patterns in a workspace region dependent manner. This hypothesis should be tested experimentally. Similarly, peripheral haptic information has been shown in preliminary phase-resetting analyses to modulate the timing structure of rhythmic speech sequences, thus supporting the hypothesis of an underlying timing network for speech that is bidirectionally coupled with, yet functionally distinct from, the dynamics of the peripheral articulatory apparatus (see also Turvey et al. 1989). More data is needed, however, not only to corroborate these findings but to generalize them beyond the production of the relatively simple, repetitive bilabial sequences that were described in this report.

References

Abraham, R. and C. Shaw, 1982. Dynamics – The geometry of behavior. Part 1: Periodic behavior. Santa Cruz, CA: Aerial Press.

Abraham, R. and C. Shaw, 1986. 'Dynamics: A visual introduction'. In F.E. Yates (ed.), Self-organizing systems: The emergence of order. New York: Plenum Press.

Beek, P.J., 1989. Juggling dynamics. Amsterdam: Free University Press.

Beek, P.J. and W.J. Beek, 1988. Tools for constructing dynamical models of rhythmic movement. Human Movement Science 7, 301–342.

Bernstein, N.A., 1967. The coordination and regulation of movements. London: Pergamon Press. Reprinted in H.T.A. Whiting (ed.), 1984. Human motor actions: Bernstein reassessed. New York: Elsevier.

Glass, L.G. and M.C. Mackey, 1988. From clocks to chaos: The rhythms of life. Princeton, NJ: Princeton University Press.

Gracco, V.L. and J.H. Abbs, 1989. Sensorimotor characteristics of speech motor sequences. Experimental Brain Research 75, 586–598.

Kawato, M., 1981. Transient and steady state phase response curves of limit cycle oscillators. Journal of Mathematical Biology 12, 13–30.

Kay, B.A., 1986. Dynamic modeling of rhythmic limb movements: Converging on a description of the component oscillators. Unpublished doctoral dissertation, Department of Psychology, Universtiy of Connecticut, Storrs, CT.

Kay, B.A., J.A.S. Kelso, E.L. Saltzman and G. Schöner, 1987. Space-time behavior of single and bimanual rhythmical movements: Data and limit cycle model. Journal of Experimental Psychology: Human Perception and Performance 13, 178–192.

Kay, B.A., E.L. Saltzman, J.A.S. Kelso, 1991. Steady-state and perturbed rhythmical movements: A dynamical analysis. Journal of Experimental Psychology: Human Perception and Performance 17, 183–197.

Lee, R.G. and R.B. Stein, 1981. Resetting of tremor by mechanical perturbations: A comparison of essential tremor and Parkinsonian tremor. Annals of Neurology 10, 523–531.

Lennard, P.R. and J.W. Hermanson, 1985. Central reflex modulation during locomotion. Trends in Neuroscience 8, 483–486.

Linkens, D.A., 1983. Integer-ratio entrainment in mutually-coupled non-linear oscillators. Journal of Theoretical Biology 101, 599–617.

Saltzman, E.L., 1979. Levels of sensorimotor representation. Journal of Mathematical Psychology 20, 91–163.

Saltzman, E. and J.A.S. Kelso, 1987. Skilled actions: A task dynamic approach. Psychological Review 94, 84–106.

Saltzman, E.L. and K.G. Munhall, 1989. A dynamical approach to gestural patterning in speech production. Ecological Psychology 1, 333–382.

Saltzman, E.L., B.A. Kay, J. Kinsella-Shaw and P.E. Rubin, in preparation. Temporal structure in short and extended speech sequences: Perturbation analyses.

Thompson, J.M.T. and H.B. Stewart, 1986. Nonlinear dynamics and chaos: Geometrical methods for engineers and scientists. New York: Wiley.

Thomson, W.T., 1981. Theory of vibration with applications (2nd ed.). Englewood Cliffs, NJ: Prentice-Hall.

Turvey, M.T., R.C. Schmidt and L.D. Rosenblum, 1989. 'Clock' and 'motor' components in absolute coordination of rhythmic movements. Neuroscience 33, 1–10.

Winfree, A.T., 1980. The geometry of biological time. New York: Springer-Verlag.